Geosci. Instrum. Method. Data Syst. Discuss., 4, 109–164, 2014
www.geosci-instrum-method-data-syst-discuss.net/4/109/2014/
doi:10.5194/gid-4-109-2014

Geoscientific Instrumentation Methods and Data Systems
Open Access
Discussions

Determining the focal mechanisms of the events in the Carpathian region of Ukraine

A. Pavlova, O. Hrytsai, and D. Malytskyy

Carpatian Branch of the Institute of Geophysics named after S.I. Subbotin NAS of Ukraine, Lviv, Ukraine

Received: 24 December 2013 – Accepted: 16 February 2014 – Published: 5 March 2014

Correspondence to: A. Pavlova (susyinet@gmail.com)

Published by Copernicus Publications on behalf of the European Geosciences Union.

Abstract

The modification of the matrix method for constructing the displacement field on the free surface of an anisotropic layered medium is presented. The source of seismic waves is modelled by a randomly oriented force and seismic tensor. A trial and error method is presented for solving the inverse problem of determining parameters of the earthquake source. A number of analytical and numerical approaches to determining the earthquake source parameters, based on the direct problem solutions, are proposed. The focal mechanisms for the events in the Carpathian region of Ukraine are determined by the graphical method. The theory of determinating the angles of orientation of the fault plane and the earthquake's focal mechanism is presented. The focal mechanisms obtained by two different methods are compared.

1 Introduction

The main data sources in seismology are the seismic records of natural or man-made events that are received on the Earth surface. The task of modern seismic analysis is to obtain the maximum possible information about the nature of wave-fields propagation. Solving these problems involves the study of seismic regions of Ukraine and interpretation of wave fields in order to determine the earthquake focal mechanisms.

In recent years one of the most important methods is the development of approaches for constructing the theoretical seismograms, which allow the study of the structure of the medium and determination of the earthquake source parameters. The effects on the wave field and seismic waves' propagation in the Earth's interior should be considered when calculating these seismograms. Thus, the displacement field, which is registered on the free surface of an inhomogeneous medium, depends on the model of the geological structure and the physical processes in the source.

Interpretation of seismic research can predict the dynamic properties of elastic media, and consider the effects of anisotropy in the inversion problems of determining the source parameters. Therefore, the problem of mathematical modelling of seismic wave propagation in anisotropic medium is relevant. Over the past decade the considerable experience in theoretical and algorithmic solutions of a wide range of dynamic seismology problems is accumulated. There are plenty of methods for solving such problems, which are quite effectively used in geophysics, including seismology. Analytical problem solving methods are developed only for a relatively narrow range of tasks. More precise, and hence more complex mathematical models are implemented by numerical methods. The last give a solution only in certain limited areas of model medium, and this is the main drawback of numerical methods. This means that the use of numerical methods, including finite difference method (Alfold, 1974; Fuchs, 1977; Ilan, 1975; Bullen, 1953; Yang, 2002; Zahradnik, 1975) and finite element method (Thomson, 1950; Woodhouse, 1978) for modelling of seismic wave propagation in inhomogeneous anisotropic media gives very high accuracy results, but requires a grid which covers the entire area occupied by the investigated object and a significant amount of computer resources for the solution of highdimensional systems of algebraic equations. Therefore, it is difficult to implement, even with the use of modern computational tools, including clusters. The matrix method is used to obtain solutions, which avoid the complicated procedures to satisfy all boundary conditions. The usefulness of solutions obtained by this method is considered in (Babuska, 1981; Bachman, 1979; Backus, 1962; Behrens, 1967; Dunkin, 1965). The matrix method allows for a common approach to examine the propagation of waves in a wide class of systems. This method allows to obtain solutions in a more compact and convenient form for further analytical and numerical calculations.

In the 50's of 20th century Thomson and Haskell first proposed a method for constructing interference fields by simulation of elastic waves in layered isotropic half-space with planar boundaries (Haskell, 1953).The matrix method was developed in the works (Malytskyy, 1998, 2008, 2010; Kennett, 1972; Cerveny, 2001; Chapman, 2004). The stable algorithms of seismograms calculation for all angles of seismic wave's propagation are obtained. The matrix method is generalized for low-frequency waves in inhomogeneous elastic concentric cylindrical and spherical layers surrounded by an

GID
4, 109–164, 2014

elastic medium. The concept of the characteristic matrix determined by physical parameters of the environment is developed. The matrix method is used for seismic waves propagation in elastic, liquid and thermoelastic media. In addition, it has been generalized for the study of other processes described by linear equations. The advantage of the matrix method is the ability to compactly write matrix expressions that are useful both in analytical studies and numerical calculations.

The matrix method and its modifications are used to simulate the seismic waves‘ propagation in isotropic and anisotropic media. This method is quite comfortable and has several advantages over other approaches. Both advantages and disadvantages of the matrix method are well described in (Malytskyy, 2010; Thomson, 1950, 1966; Ursin, 1983).

Today in seismology much attention is given to mathematical modelling as one of the main tools for the analysis and interpretation of the wave fields. In this paper using a modification of the matrix method Thomson–Haskell, rigorous equations for the wave field on the free surface of inhomogeneous anisotropic medium are obtained, when a source of seismic waves is located within a homogeneous anisotropic layer and presented by the seismic moment tensor. Note that the problem of wave fields modelling generated by a source, which is presented in terms of seismic moment tensor, also has practical applications in seismology. Using this method, the approaches to determining the displacement field are developed for different types of earthquake sources that will be shown in the following sections.

2 Direct problem

The problem of wave fields modelling, when the source is presented by seismic tensor moment, has practical applications in seismology. Therefore, the development of methods for determining the displacement field on the free surface of an anisotropic inhomogeneous medium for sources of this type is an actual task and needs to be resolved.

In this section the propagation of seismic waves in inhomogeneous anisotropic medium is considered. The modification of the matrix method of construction of wavefield on the free surface of an anisotropic medium is presented. The earthquake source represented by a randomly oriented force or a seismic moment tensor is placed on an arbitrary boundary of a layered anisotropic medium. The theory of the matrix propagator in a homogeneous anisotropic medium by introducing a “wave propagator” is presented. It is shown that for anisotropic layered medium the matrix propagator can be represented by a “wave propagator” in each layer. The displacement field on the free surface of an anisotropic medium is obtained from the received system of equations considering the radiation condition and that the free surface is stressless.

2.1 Theory of modification of the matrix method

The problem of wave fields modelling, when the source is presented by seismic moment, has practical applications in seismology. Therefore, the development of methods for determining the displacement field on the free surface of an anisotropic inhomogeneous medium for sources of this type is an actual task and needs to be resolved.

In this paper the propagation of seismic waves in anisotropic inhomogeneous medium is modelled by system of homogeneous anisotropic layers, as shown in (Fig. 1). The each layer is characterized by the propagation velocity of P and S wave and density. At the boundaries between layers hard contact condition is met, except for the border, where the source of seismic waves is located.

The earthquake source is modelled by nine pairs of forces, which represented a seismic moment tensor. This description of the point source is sufficiently known and effective for simulation of seismic waves in layered half-space (Haskell, 1953). In general, the source is also assumed to be distributed over time, i.e. seismic moment $M_0(t)$ is a function of time. This means that the physical process in the source does not occur instantaneously, but within a certain time frame. It is known for our seismic events (Mw ∼ 2–3) that the time during which occurred the event may be 0.1–0.7 s. The determination of the source time function is an important seismic problem. In this chapter the direct problem solution is shown, when a point source is located on an arbitrary boundary of layered anisotropic media.

We assume the usual linear relationship between stress τ_{ij} and strain e_{kl}

$$\boldsymbol{\tau}_{ij} = \mathbf{c}_{ijkl} \cdot \mathbf{e}_{kl} = \mathbf{c}_{ijkl} \frac{\partial u_l}{\partial x_k} \tag{1}$$

where $\boldsymbol{u} = (u_x, u_y, u_z)^T$ is displacement vector.

The equation of motion for an elastic homogeneous anisotropic medium, in the absence of body forces is (Fryer et al., 1984)

$$\rho \frac{\partial^2 u_i}{\partial t^2} = \mathbf{c}_{ijkl} \frac{\partial^2 u_l}{\partial x_j \partial x_k} \tag{2}$$

where ρ is the uniform mass density, and c_{ijkl} are the elements of the uniform elastic coefficient tensor.

Taking the Fourier transform of Eqs. (1) and (2), we obtain the matrix equation (Fryer et al, 1987)

$$\frac{\partial \boldsymbol{b}}{\partial z} = j\varpi \mathbf{A}(z)\boldsymbol{b}(z) \tag{3}$$

where $\boldsymbol{b} = \begin{pmatrix} \boldsymbol{u} \\ \tau \end{pmatrix}$ is the vector of displacements and scaled tractions, $\boldsymbol{\tau} = -\frac{1}{j\varpi}(\tau_{xz}, \tau_{yz}, \tau_{zz})^T$. With the definition of $\boldsymbol{b}$ the system matrix $\mathbf{A}$ has the structure $\mathbf{A} = \begin{pmatrix} \mathbf{T} & \mathbf{C} \\ \mathbf{S} & \mathbf{T}^{\mathrm{T}} \end{pmatrix}$; where $\mathbf{T}$, $\mathbf{S}$ and $\mathbf{C}$ are 3×3 sub matrices, $\mathbf{C}$ and $\mathbf{S}$ are symmetric.

For any vertically stratified medium, the differential system Eq. (3) can be solved subject to specified boundary conditions to obtain the response vector $\boldsymbol{b}$ at any desired depth. If the response at depth z_0 is $\boldsymbol{b}(z_0)$, the response at depth z is

$$\boldsymbol{b}(z) = \mathbf{P}(z, z_0)\boldsymbol{b}(z_0) \tag{4}$$

GID
4, 109–164, 2014

where $P(z,z_0)$ is the stress-displacement propagator.

To find this propagator, it is necessary to find the eigenvalues (vertical slownesses), the eigenvector matrix $\mathbf{D}$, and its inverse $\mathbf{D}^{-1}$ (Fryer et al., 1984):

$$\mathbf{P}(z,z_1) = \mathbf{DQ}(z,z_1)\mathbf{D}^{-1}, \quad (5)$$

where $\mathbf{Q}$ is the "wave" propagator (Fryer et al., 1984):

$$\mathbf{Q}(z,z_1) = \begin{pmatrix} \mathbf{E}_u & 0 \\ 0 & \mathbf{E}_D \end{pmatrix} \quad (6)$$

where $\mathbf{E}_u = \mathrm{diag}[e^{j\omega(z-z_1)q_p^u}, e^{j\omega(z-z_1)q_{s_1}^u}, e^{j\omega(z-z_1)q_{s_2}^u}]$, $\mathbf{E_D} = \mathrm{diag}[e^{j\omega(z-z_1)q_p^D}, e^{j\omega(z-z_1)q_{s_1}^D}, e^{j\omega(z-z_1)q_{s_2}^D}]$. In the isotropic case the eigenvector matrix $\mathbf{D}$ known analytically, so the construction of the propagator is straightforward. In the anisotropic case, analytic solutions have been found only for simple symmetries so in general, solutions will be found numerically.

The layered anisotropic medium, which consists of n homogeneous anisotropic layers on an anisotropic halfspace $(n+1)$ (Fig. 1), is considered. The source in the form of a jump in the displacement-stress $F = \boldsymbol{b}_{s+1} - \boldsymbol{b}_s$ is placed on the s-boundary (Fig. 1); it is easy to write the following matrix equation, using Eqs. (5) and (6):

$$\boldsymbol{b}_{n+1} = \mathbf{P}_{n,s}\boldsymbol{b}_{s+1}|_{z=z_s}, \boldsymbol{v}_{n+1} = \mathbf{D}_{n+1}^{-1}\mathbf{D}_n\mathbf{Q}_n\mathbf{D}_n^{-1}\cdots\mathbf{D}_{s+1}\mathbf{Q}_{s+1}\mathbf{D}_{s+1}^{-1}\cdot\boldsymbol{b}_{s+1}|_{z=z_s},$$
$$\boldsymbol{b}_s|_{z=z_s} = \mathbf{P}_{s,s-1}\mathbf{P}_{s-1,s-2}\cdots\mathbf{P}_{2,1}\mathbf{P}_{1,0}\cdot\boldsymbol{b}_0 = \mathbf{D}_s\mathbf{Q}_s\mathbf{D}_s^{-1}\cdots\mathbf{D}_1\mathbf{Q}_1\mathbf{D}_1^{-1}\cdot\boldsymbol{b}_0,$$
$$\boldsymbol{v}_{n+1} = \mathbf{D}_n\mathbf{Q}_n\mathbf{D}_n^{-1}\cdots\mathbf{D}_{s+1}\mathbf{Q}_{s+1}\mathbf{D}_{s+1}^{-1}\cdot(\boldsymbol{b}_s + F)$$
$$= \mathbf{G}^{n+1,s+1}\cdot(\mathbf{G}_{s,1}\boldsymbol{b}_0 + F) = \mathbf{G}^{n+1,s+1}\mathbf{G}_{s,1}\boldsymbol{b}_0 + \mathbf{G}^{n+1,s+1}\cdot F = \mathbf{G}\boldsymbol{b}_0 + \mathbf{G}^{n+1,s+1}\cdot F,$$

where

$$\mathbf{G} = \mathbf{D}_{n+1}^{-1}\mathbf{D}_n\mathbf{Q}_n\mathbf{D}_n^{-1}\cdots\mathbf{D}_{s+1}\mathbf{Q}_{s+1}\mathbf{D}_{s+1}^{-1}\cdots\mathbf{D}_2^{-1}\mathbf{D}_1\mathbf{Q}_1\mathbf{D}_1^{-1}$$

GID
4, 109–164, 2014

– characteristic matrix of a layered anisotropic medium.

$$\boldsymbol{v}_{n+1} = \mathbf{G}\boldsymbol{b}_0 + \mathbf{G}\cdot\mathbf{G}_{s,1}^{-1}\cdot \boldsymbol{F} = \mathbf{G}(\boldsymbol{b}_0 + \mathbf{G}_{s,1}^{-1}\cdot \boldsymbol{F}) = \mathbf{G}(\boldsymbol{b}_0 + \tilde{\boldsymbol{F}}), \tag{7}$$

where $\tilde{\boldsymbol{F}} = \mathbf{G}_{s,1}^{-1}\cdot \boldsymbol{F}$, $\mathbf{G} = \mathbf{G}^{n+1,s+1}\cdot \mathbf{G}_{s,1}$.

Using Eq. (7) and the radiation condition (with a halfspace (n+1) the waves are not returned), and also the fact that the tension on the free surface equals to zero, we obtain a system of equations:

$$\begin{pmatrix} 0 \\ 0 \\ 0 \\ v_D^P \\ v_D^{S_1} \\ v_D^{S_2} \end{pmatrix} = \begin{pmatrix} G_{11} & G_{12} & G_{13} & G_{14} & G_{15} & G_{16} \\ G_{21} & G_{22} & G_{23} & G_{24} & G_{25} & G_{26} \\ G_{31} & G_{32} & G_{33} & G_{34} & G_{35} & G_{36} \\ G_{41} & G_{42} & G_{43} & G_{44} & G_{45} & G_{46} \\ G_{51} & G_{52} & G_{53} & G_{54} & G_{55} & G_{56} \\ G_{61} & G_{62} & G_{63} & G_{64} & G_{65} & G_{66} \end{pmatrix} \begin{pmatrix} u_x^{(0)} + \tilde{F}_1 \\ u_y^{(0)} + \tilde{F}_2 \\ u_z^{(0)} + \tilde{F}_3 \\ \tilde{F}_4 \\ \tilde{F}_5 \\ \tilde{F}_6 \end{pmatrix}.$$

Using only the homogeneous equations is sufficient to get the displacement field on a free surface:

$$\begin{cases} G_{11}u_x^{(0)} + G_{12}u_y^{(0)} + G_{13}u_z^{(0)} = -(G_{11}\tilde{F}_1 + G_{12}\tilde{F}_2 + G_{13}\tilde{F}_3 + G_{14}\tilde{F}_4 + G_{15}\tilde{F}_5 + G_{16}\tilde{F}_6) \\ G_{21}u_x^{(0)} + G_{22}u_y^{(0)} + G_{23}u_z^{(0)} = -(G_{21}\tilde{F}_1 + G_{22}\tilde{F}_2 + G_{23}\tilde{F}_3 + G_{24}\tilde{F}_4 + G_{25}\tilde{F}_5 + G_{26}\tilde{F}_6) \\ G_{31}u_x^{(0)} + G_{32}u_y^{(0)} + G_{33}u_z^{(0)} = -(G_{31}\tilde{F}_1 + G_{32}\tilde{F}_2 + G_{33}\tilde{F}_3 + G_{34}\tilde{F}_4 + G_{35}\tilde{F}_5 + G_{36}\tilde{F}_6) \end{cases}$$

GID
4, 109–164, 2014
Determining the focal mechanisms
A. Pavlova et al.

The stress-displacement discontinuity is determined via the seismic in matrix form (Fryer et al., 1984):

$$\boldsymbol{F} = \begin{pmatrix} -c_{55}^{-1} M_{xz} \\ -c_{44}^{-1} M_{yz} \\ -c_{33}^{-1} M_{zz} \\ p_x (M_{xx} - c_{13} c_{33}^{-1} M_{zz}) + p_y M_{xy} \\ p_x M_{yx} + p_y (M_{yy} - c_{23} c_{33}^{-1} M_{zz}) \\ p_x (M_{zx} - M_{xz}) + p_y (M_{zy} - M_{yz}) \end{pmatrix} \delta(z - z_z) \tag{8}$$

where M_{xx}, M_{yy}, M_{zz}, M_{xz}, M_{yz}, M_{yx}, M_{xy}, M_{zy}, M_{zx} – components of the seismic moment tensor, and c_{13}, c_{23}, c_{33}, c_{44}, c_{55} – components of the stiffness matrix.

As a result, the displacement field of the free surface of an anisotropic medium is in the spectral domain as (Malytskyy, 2013b):

$$\boldsymbol{u} = \begin{pmatrix} u_x^0 \\ u_y^0 \\ u_z^0 \end{pmatrix} = (\mathbf{G}^{13})^{-1} \cdot \boldsymbol{y}, \tag{9}$$

where

$$\mathbf{G}^{13} = \begin{pmatrix} G_{11} & G_{12} & G_{13} \\ G_{21} & G_{22} & G_{23} \\ G_{31} & G_{32} & G_{33} \end{pmatrix}, \quad \boldsymbol{y} = \begin{pmatrix} a \\ b \\ c \end{pmatrix},$$

$$a = -(G_{11}\tilde{F}_1 + G_{12}\tilde{F}_2 + G_{13}\tilde{F}_3 + G_{14}\tilde{F}_4 + G_{15}\tilde{F}_5 + G_{16}\tilde{F}_6),$$

$$b = -(G_{21}\tilde{F}_1 + G_{22}\tilde{F}_2 + G_{23}\tilde{F}_3 + G_{24}\tilde{F}_4 + G_{25}\tilde{F}_5 + G_{26}\tilde{F}_6),$$

$$c = -(G_{31}\tilde{F}_1 + G_{32}\tilde{F}_2 + G_{33}\tilde{F}_3 + G_{34}\tilde{F}_4 + G_{35}\tilde{F}_5 + G_{36}\tilde{F}_6).$$

Using Eq. (9) and three-dimensional Fourier transform, we obtain a direct problem solution for the displacement field of the free surface of an anisotropic medium in the

GID
4, 109–164, 2014

time domain as:

$$\boldsymbol{u}(x,y,z_R,t) = \frac{1}{8\pi^3}\iiint\limits_{-\infty} \varpi^2 \boldsymbol{u}(p_x,p_y,z_R,\varpi)e^{j\varpi(t-p_x x-p_y y)}\mathrm{d}p_x \mathrm{d}p_y \mathrm{d}\varpi, \quad (10)$$

where z_R – epicentral distance, p_x,p_y – horizontal slowness.

3 Inverse problem

It is known that inverse problems are inherently incorrect. In seismology methods and approaches often are used, which are reduced to the selection of the physical characteristics of the studied environment or earthquake (Brace, 1966, 1978; Clinton, 2006; Cohn, 1982; Hartzell, 1979; Santosa, 1986; Choy, 1981; Hanks, 1979; Honda, 1957, 1962; Scholz, 1973). The development of new methods and algorithms for determining of source parameters is relevant and important issue. Of course, there is not general and reliable approach. Furthermore, it is impossible to consider all effects in modelling wave processes during propagation of seismic waves in heterogeneous environments. Therefore, for an anisotropic medium it is difficult to construct a theory that would be based only on analytical expressions. Thus, we must resort to numerical solution of equations.

3.1 Traditional graphical method and trial and error method for determining of the earthquake source parameters

The focal mechanism solution for earthquakes in the region of low seismic activity today is the actual problem. Particularly it is very important for Carpathian region of Ukraine, where insufficient number of stations is in addition to low seismic activity. It is impossible to determine a focal mechanism by software packages.

The software packages Matlab 7.12.0 (R2011a) is used for programming in this paper. Algorithms and software of the direct dynamic problem solving is based on the method described in Sect. 2.1. This method is based on the use of matrix and wave propagators, which are applied to inhomogeneous anisotropic media modelled by bundle of homogeneous anisotropic layers with parallel boundaries. Algorithm for calculating the displacement field on free surface of a layered anisotropic medium in the Cartesian coordinate system $\left(u_x^{(0)}, u_y^{(0)}, u_z^{(0)}\right)$ is based on certain physical and mathematical constraints:

1. heterogeneous anisotropic medium is modelled by a bundle of homogeneous anisotropic layers;
2. homogeneous anisotropic layers are separated by parallel boundaries;
3. contact between the layers is considered hard (continuity of displacements and stresses);
4. a point source is located within any homogeneous anisotropic layer.

Thus, the algorithm for calculating the displacement field on free surface of a layered anisotropic medium defined by Eq. (10) in the Cartesian coordinate system. The equations for the direct dynamic problem are obtained by means of numerical calculations.

In the algorithms and programs is used Fast Fourier Transform (FFT) to the variables (t, ω). Maximum frequency, step frequency and sampling time were chosen from the conditions:

$$\omega_{max} = 2\pi f_{max},$$

where

$$\Delta t = \frac{1}{2f_{max}}; \Delta f = \frac{f_{max}}{2^n} (n = 10).$$

Waves are excited by a point source, represented by seismic moment tensor. The relationship between the components of the seismic moment tensor and fault plane orientation angles is given as (Aki, 2002):

$$
\begin{aligned}
M_{xx} &= -M_0(\sin\delta\cos\lambda\sin 2\phi_s + \sin 2\delta\sin\lambda\sin^2\phi_s) \\
M_{xy} &= M_0(\sin\delta\cos\lambda\cos 2\phi_s + 1/2\sin 2\delta\sin\lambda\sin 2\phi_s) \\
M_{xz} &= -M_0\ (\cos\delta\cos\lambda\cos\phi_s\ +\ \cos 2\delta\sin\lambda\sin\phi_s)\ =\ M_{zx} \\
M_{yy} &= \ M_0\ \left(\sin\delta\cos\lambda\sin 2\phi_s\ -\ \sin 2\delta\sin\lambda\cos^2\phi_s\right) \\
M_{yz} &= -M_0\ (\cos\delta\cos\lambda\sin\phi_s\ -\ \cos 2\delta\sin\lambda\cos\phi_s)\ = M_{zy} \\
M_{zz} &= -M_0\ \sin 2\delta\sin\lambda
\end{aligned}
\tag{11}
$$

where $M_0 = \mu\text{Au}(\tau)$ – seismic moment; δ – a dip angle; ϕ_s– a strike angle; λ – a slip angle.

The tensor Eq. (11) is defined by the geometric orientation of the fault plane and the value of seismic moment M_0.

Obtaining of the analytical expressions to determine the earthquake source parameters, when the source is represented by seismic moment tensor, is difficult. The most accurate results of the inverse problem solving for the source parameters are obtained by the trial and error method. In this method, the synthetic seismograms are calculated many times for all possible combinations of orientation angles of the fault plane and the velocity model for the Carpathian region of Ukraine. The correlation coefficients are calculated for the all these synthetic seismograms and real record of event. The biggest correlation coefficient corresponds to the most probable combination of orientation angles of the fault plane. The best results of solving are for the records from stations in smaller epicenter distance, these records usually have the lowest noise level. The results obtained by this method are compared with results for the same event but received by graphical method (Malytskyy, 2013a).

In the trial and error method the matrix Eq. (9) is solved for the velocity model for the Carpathian region of Ukraine (Table 1) and for the stress-displacement discontinuity Eq. (8), where components of seismic tensor are determined via oriental angles of the fault plane Eq. (11).

GID

4, 109–164, 2014

The traditional graphical method based on the first arrival P waves (Malytskyy, 2013a; Bornmann, 2009; Cheng, 1992) using information about fuzzy first motion (Cronin, 2004) and the S/P amplitude ratio (Hardebeck, 2003).

The polarities first motion P waves was defined from complete records seismograms taking into account the possible inversion of the sign on the z-component. A logarithm of the amplitude ratio S/P is calculated using data from the three components seismic records of this event at each station (Hardebeck, 2003; de Natale, 1994). Input data for the azimuth and take-off angle are calculated by software packages for each event.

Most often an approach is used where nodal planes are plotted on a lower-hemisphere stereographic projection such as to best fit the polarities of first arrivals of P waves at the stations location of a station polarity on the projection depending on the station azimuth and take-off angle of the ray of first arrival connecting the source and the station.

These focal mechanisms are determined using a method that attempts to find the best fit to the direction of P wave first motions observed at each station. For a double-couple source mechanism (or only shear motion on the fault plane), the compression first-motions should lie only in the quadrant containing the tension axis, and the dilatation first-motions should lie only in the quadrant containing the pressure axis. Accuracy focal mechanism solution depends on the input data: velocity model and coordinate of the hypocenter (they determine the take-off angle), quality of seismic records and sign inversion on the seismometer, so that “up” is “down” (they determine character entry wave).

S/P amplitude ratios are applicable because of P wave amplitude being the largest on P and T axes of focal mechanism and the smallest near the nodal planes, while the S wave amplitude being the largest near the nodal planes. S/P amplitude ratios with a wide range of values can more accurately constrain the location of seismic station projections on the focal sphere. The larger S/P amplitude ratios, the closer the location of the seismic station projection to the nodal line.

Seismic moment and other spectral parameters are computed by (12–19) for each station (Bormann, 2009).

The seismic moment is computed according to:

$$M_0 = 4\pi r v_p^3 \rho u_0/(\theta S_a), \tag{12}$$

where r – hypocentral distance, v_p-P wave velocity, ρ – density, u_0 – low-frequency level (plateau) of the displacement spectrum, Θ – average radiation pattern and S_a surface amplification for P waves.

The source radius R is computed from the relationship:

$$R = \frac{3.36 v_p}{2\sqrt{3}\pi f_c}, \tag{13}$$

where f_c – corner frequency of the P wave.

The size of the circular rupture plane is computed as:

$$A = \pi R^2 \tag{14}$$

The average source dislocation is according to

$$\overline{D} = M_0/\mu A, \tag{15}$$

where the shear modulus computed by

$$\mu = v_p^2 \rho/3. \tag{16}$$

The stress drop, seismic energy and magnitude ML are computed according to:

$$\Delta\sigma = 7M_0/16R^3, \tag{17}$$

$$E_s = M_0 \cdot 1.6 \cdot 10^{-5}, \tag{18}$$

$$\mathrm{ML} = (\lg E_s - 4)/1.8. \tag{19}$$

GID
4, 109–164, 2014

3.2 Determining the parameters of earthquake sources

In approving the proposed trial and error method for determining of the earthquake source parameters the four events in the Carpathian region of Ukraine were considered. For each of these events an earthquake focal mechanism is determined by the method of selection and graphical method. These focal mechanisms are compared.

1. The earthquake took place on the district NNP "Synevyr" the Carpathian region of Ukraine ($\phi = 48.5309^\circ$, $\lambda = 23.8365^\circ$, ML = 1.96), 2012.01.06 at 04:34:10.464 at the depth 5 km.

Taking into account the S/P amplitude ratio (Table 2) the most probable focal mechanism is chosen.

The seismic tensor corresponds to the focal mechanism (Fig. 3) which is defined by the graphical method:

$$\mathbf{M} = \begin{pmatrix} -14.932 & 0.528 & -13.361 \\ 0.528 & 3.426 & 9.457 \\ -13.361 & 9.457 & 11.506 \end{pmatrix} \times 10^{11}$$

The focal mechanism is also determined by the trial and error method. Using the velocity model for the Carpathian region of Ukraine (Table 1), the wavefield on a free surface is calculated many times for all combination of dip, strike and slip angles. All of these synthetic seismograms are compared with real records of this event. The correlation coefficients are calculated for all of these synthetic waveforms and real seismograms. The largest coefficient corresponds to the most probable combination of fault plane orientation angles. The largest correlation coefficient R is equal to 0.8495 for the earthquake, which took place near NNP "Synevyr" on 6 January 2012. On Fig. 4 the coefficients R for synthetic and real seismograms are shown. On the horizontal axis a nodal plane identifier (combinations of dip, strike and slip angles) is plotted.

The maximum coefficient R corresponds to the focal mechanism, which is shown on Fig. 5.

GID
4, 109–164, 2014

Seismic tensor corresponds to the focal mechanism (Fig. 5) which is defined by the trial and error method:

$$\mathbf{M} = \begin{pmatrix} -8.27 & -0.27 & -18.55 \\ -0.27 & 1.13 & 6.86 \\ -18.55 & 6.86 & 7.14 \end{pmatrix} \times 10^{11}$$

Obtained focal mechanisms (Figs. 3b and 5) by two different methods are very similar, so we can assume that these solutions of this earthquake are correct.

2. The earthquake took place on the district NNP "Synevyr" the Carpathian region of Ukraine ($\phi = 48.5367°$, $\lambda = 23.8378°$, ML = 2.23), 10 January 2012 at 12:12:55584 at the depth 5.7 km.

Taking into account the ratio of P and S waves amplitudes (Table 6) and waveforms similarity with the event 10 January 2010 choose as the most probable focal mechanism:

Seismic tensor corresponds to the focal mechanism (Fig. 7) which is defined by the graphical method:

$$\mathbf{M} = \begin{pmatrix} -46.632 & 0.672 & -37.179 \\ 0.672 & 0.625 & 27.846 \\ -37.179 & 27.846 & 40.381 \end{pmatrix} \times 10^{11}$$

The focal mechanism is also determined by described above the trial and error method. Similarly to the previous case the synthetic seismograms and correlation coefficients are calculated. The largest correlation coefficient R is equal 0.9524 for the earthquake, which took place near NNP "Synevyr" on 10 January 2012. On Fig. 8 the coefficients R for synthetic and real seismograms are shown.

The maximum correlation coefficient R corresponds to the focal mechanism, which is shown on Fig. 9.

GID
4, 109–164, 2014

Seismic tensor corresponds to the focal mechanism (Fig. 9) which is defined by the trial and error method:

$$\mathbf{M} = \begin{pmatrix} -24.74 & -2.78 & -57.38 \\ -2.78 & 3.17 & 16.77 \\ -57.38 & 16.77 & 21.57 \end{pmatrix} \times 10^{11}$$

Obtained focal mechanisms (Figs. 7b and 9) by two different methods are very similar, so we can assume that these solutions of this earthquake are correct.

3. The earthquake took place near village Ugla ($\phi = 48.1676^\circ$, $\lambda = 23.6525^\circ$, ML = 1.92), 24 October 2012 at 03:13:40501 at the depth 5 km

Taking into account the S/P amplitude ratio (Table 10) the most probable focal mechanism is chosen.

Seismic tensor corresponds to the focal mechanism (Fig. 11):

$$\mathbf{M} = \begin{pmatrix} -1.8632 & -6.2485 & -9.9630 \\ -6.2485 & -10.9449 & -7.6925 \\ -9.9630 & -7.6925 & 12.8082 \end{pmatrix} \times 10^{11}$$

Obtained focal mechanism by the graphical method is compared with the trial and error method results for the event near village Ugla (24 October 2012). The correlation coefficients are calculated by the trial and error method described above. The largest coefficient R is equal 0.9788 and corresponds to the focal mechanism, which is shown on Fig. 13.

Seismic tensor corresponds to the focal mechanism (Fig. 13) which is defined by the trial and error method:

$$\mathbf{M} = \begin{pmatrix} -2.22 & -7.10 & 12.06 \\ -7.10 & -9.06 & -6.19 \\ 12.06 & -6.19 & 11.28 \end{pmatrix} \times 10^{11}$$

Obtained focal mechanisms (Figs. 11b and 13) by two different methods are very similar, so we can assume that these solutions of this earthquake are correct.

4. The earthquake took place near village Nyzhnje Selyshche ($\phi = 48.1977^\circ$, λ=23.4663°, ML = 2.22), 4 April 2013 at 21:15:1436 at the depth 1.8 km.

Taking into account the S/P amplitude ratio (Table 14) the most probable focal mechanism is chosen. Seismic tensor which corresponds to the focal mechanism (Fig. 15):

$$\mathbf{M} = \begin{pmatrix} -11.42494 & -54.24707 & -54.15575 \\ -54.24707 & 1.96935 & 5.69199 \\ -54.15575 & 5.69199 & 9.45559 \end{pmatrix} \times 10^{11}$$

Obtained focal mechanism by the graphical method is compared with the trial and error method results for the event near village Nyzhnje Selyshche (4 April 2013). The correlation coefficients are calculated by the trial and error method described above. The largest coefficient R is equal 0.7400 and corresponds to the focal mechanism, which is shown on Fig. 17.

Seismic tensor corresponds to the focal mechanism (Fig. 17) which is defined by the trial and error method:

$$\mathbf{M} = \begin{pmatrix} -9.51 & -44.99 & -48.55 \\ -44.99 & 4.86 & 4.78 \\ -48.55 & 4.78 & 4.65 \end{pmatrix} \times 10^{11}$$

Obtained focal mechanisms (Figs. 15b and 17) by two different methods are very similar, so we can assume that these solutions of this earthquake are correct.

4 Conclusion

The results of this paper contribute to the fundamental understanding of wave propagation in anisotropic media. A numerical technique for computing synthetic seismograms

GID
4, 109–164, 2014

has been developed in the framework of the theory. Wave propagation in multilayered media requires that displacement and stress vectors be continuous everywhere, including the interfaces.

Seismologists have been able to invert the rupture process of a number of earthquakes and many of the features predicted by simple dynamic source models have been quantified and observed. Foremost among these is the shape of the FF spectrum, the basic scaling laws relating particle velocity and acceleration to properties of the fault, such as size, stress drop and rupture velocity. Recent inversions of earthquake slip distributions using kinematic source models have found very complex source distributions that require an extensive reappraisal of classical source models. It is shown that the developed method for determining the earthquake parameters can be used successfully using real records. It should be also noted that the proposed method for determining the seismic moment tensor can be used in seismology for a class of problems, when the velocity model of the medium is known. Thus, the methods, approaches, algorithms, software for the propagation of seismic waves and results of direct and inverse dynamic problems of seismology proposed and developed by the authors and highlighted in the paper, can be successfully used in the study of the seismic regions and effective implementation in the construction of the earthquake source mechanism which is crucial for seismic regions of the country.

The focal mechanisms are determined also using the graphical method, which based on the first arrival P waves, information about fuzzy first motion and the S/P amplitude ratio.

References

Aki, K. and Richards, P. G.: Quantitative Seismology, 2nd Edn., University Science Books, Sausalito, California, 2002.

Alford, R. M., Kelly, K. R., and Boore, D. M.: Accuracy of finite difference modeling of the acoustic wave equation, Geophysics, 39, 834–842, 1974.

Auld, B. A.: Acoustic fields and waves in solids, J. Wiley and Sons, New York, 18 pp., 1973.
Babuska, V.: Anisotropy of Vp and Vs in rock-forming minerals, Geophys. J. R. Astr. Soc, 50, 1–6., 1981.
Bachman, R. T.: Acoustic anisotropy in marine sediments and sedimentary rocks, J. Geophys. Res., 84, 7661–7663, 1979.
Backus, G. E.: Long-wave elastic anisotropy produced by horizontal layering, J. Geophys. Res., 67, 4427–4440, doi:10.1029/JZ067i011p04427, 1962.
Behrens, E.: Sound propagation in lamellar composite materials and averaged elastic constants, J. Acoust. Soc. Am., 42, 168–191, 1967.
Bormann, P.: New Manual of Seismological Observatory Practice, Potsdam: Deutsches GeoForschungsZentrum GFZ, 2009.
Brace, W. F. and Byerlee, J. D.: Stick-slip as a mechanism for earthquake, Science, 153, 990–992, 1966.
Brace, W. F.: Volume changes during fracture and frictional sliding, a rev., Pure Appl. Geophys., 116, 603–614, 1978.
Bullen, K. E.: On strain energy in Earth's upper mantle, Trans. Amer. Geoph. Union, 34, 107–116., 1953.
Cerveny, V.: Seismic Ray Theory, Cambridge, Cambridge University Press, 2001.
Chapman, C. H.: Fundamentals of Seismic Wave Propagation, Cambridge, Cambridge University Press, 608 pp., 2004.
Cheng, S., Hron, F., and Daley, P. F.: Determination of shear wave velocities and densities from *P* wave amplitudes in VSP data, Canadian Journal of Exploration Geophysics, 28, 19–29, 1992.
Choy, G. L. and Boatwright, J.: The rupture characteristics of two deep earthquakes inferred from broadband GDSN data, B. Seismol. Soc. Am., 71, 691–711, 1981.
Clinton, J. F., Hauksson, E., and Solanki, K.: An evaluation of the scan moment tensor solution: robustness of the MW Magnitude scale, style of faulting and automation of the method, B. Seismol. Soc. Am., 96, 1689–1705, 2006.
Cohn, S. N., Hong, T., and Helmberger, D. V.: The Oroville earthquakes: a study of source characteristics and site effects, J. Geophys. Res., 87, 4585–4594, 1982.
Crampin, S.: The dispertion of surface waves in multilayered anisotropic media, Geophys. J. Roy. Astron. Soc., 21, 387–402, 1970.

GID
4, 109–164, 2014
Determining the focal mechanisms
A. Pavlova et al.

Crampin, S.: A review of wave motion in anisotropic and cracked elastic-media, Wave Motion, 3, 343–391, 1981.
Cronin, V. A.: Draft Primer on Focal Mechanism Solutions for Geologists, http://serc.carleton.edu/files/NAGTWorkshops/structure04/Focal_mechanism_primer.pdf (last access: 3 March 2014), 2004.
de Natale, G.: Focal mechanism determination for volcanic microearthquakes, Ann. Geofis., 37, 1621–1643., 1994.
Dunkin, I. W.: Computation of modal solutions in layered elastic media at high frequencies, B. Seismol. Soc. Am., 55, 335–358, 1965.
Fryer, G. J. and Frazer, L. N.: Seismic waves in stratified anisotropic media, Geophys. J. R. Astr. Soc., 78, 691–710, 1984.
Fryer, G. J. and Frazer, L. N.: Seismic waves in stratified anisotropic media – II. Elastodynamic eigensolutions for some anisotropic systems, Geophys J. R., and Soc., 91, 73–101, 1987.
Fuchs, K.: Explosion seismology and the continental crust-mantle boundary, J. Geol. Soc. London, 134, 139–151, 1977.
Hanks, T. C. and Kanamori, H.: A moment-magnitude scale, J. Geophys. Res., 84, 2348–2350, 1979.
Hardebeck, J. L. and Shearer, P. M.: Using S/P amplitude ratios to constrain the focal mechanisms of small earthquakes, B. Seismol. Soc. Am., 93, 2434–2444, 2003.
Hartzell, S. H. and Heaton, T. H.: Inversion of strong ground motion and teleseismic waveform data for the fault rupture history of the 1979 Imperial Valley, California earthquake, Bull. Sersm. Soc. Am., 73, 1553–1583, 1983.
Haskell, N. A.: The dispersion of waves in multilayered media, B. Seismol. Soc. Am., 43, 17–34, 1953.
Honda, H.: The mechanism of the earthquakes, Sci. Rep. Thoku Univ., Geophysics, 9, 1–46, 1957.
Honda, H.: Earthquake mechanism and seismic waves, J. Phys/Earth, 10, 1–97, 1962.
Ilan, A., Ungar, A., and Alterman, Z. S.: An improved representation of boundary conditions in finite difference schemes for seismological problems, Geophys. J. Roy. Astron. Soc., 43, 727–745, 1975.
Kennet, B. L. N.: Seismic waves in laterally inhomogeneous media, Geophys. J. R. Astr. Soc., 27, 301–325, 1972.

Kennett, B. L. N.: Seismic Wave Propagation in Stratified Media, Cambridge Univ. Pres., Cambridge, 1983.

Kennett, B. L. N., Sambridge, M. S., and Williamson, P. R.: Subspace methods for inverse problems with multiple parameter classes, Geophys. J. Int., 94, 237–247, 1988.

Malytskyy, D.: General principles of seismological dynamic problem solution on the basis of the recurrent method, Geophysical Journal, IGF NASU, 20, 96–98, 1998.

Malytskyy, D.: Analytic-numerical approaches to the calculation of seismic moment tensor as a function of time, Geoinformatika, 1, 79–85, 2010.

Malytskyy, D. and Muyla, O.: Particularities of Modelling of Earthquake Source, Theoretical and applied aspects of Geoinformatics, 1, 304–310, 2008.

Malytskyy, D. and Pavlova, A.: Seismic wave propagation in anisotropic media, direct problem – I. Geoinformatykà, 45, 25–30, 2013.

Malytskyy, D., Hrytsai, O., and Muyla, O.: The features of the construction of the focal mechanisms of local earthquakes using the example of an event near Beregovo 23.11.2006, Visnyk KNU, Geology, 60, 37–42, 2013.

Santosa, F. and Symes, W. W.: Inverse problem for a layered acoustic wave propagation, in: Mathematical and Computational Methods in Seismic Exploration and Reservoir Modeling, edited by: Fitzgibbon, W., SIAM Publications, Philadelphia, 259–263, 1986.

Scholz, C. H., Sykes, L. R., and Aggarawal, Y. P.: Earthquake prediction: a physical basis, Science, 181, 803–810, 1973.

Thomsen, L.: Weak elastic anisotropy, Geophysics, 51, 1954–1966, 1986.

Thomson, W. T.: Transmission of elastic waves through a stratified solid medium, J. Appl. Phys., 21, 89–93, 1950.

Ursin, B.: Review of elastic and electromagnetic wave propagation in horizontally layered media, Geophysics, 48, 1063–1081., 1983.

Woodhouse, J. H.: Asymptotic results for elastodynamic propagator matrices in plane stratified and spherically stratified Earth models, Geophys. J. R. Astr. Soc., 54, 263–280, 1978.

Yang, D. H., Liu. E., Zhang, Z. J., and Teng, J.: Finite-difference modelling in two-dimensional anisotropic media using a flux-corrected transport technique, Geophys. J. Int., 148, 320–328, 2002.

Zahradnik, J.: Finite difference solutions to certain diffraction problems, Stud. Geophys. Geod., 19, 233–244, 1975.

GID
4, 109–164, 2014

Table 1. Velocity model for the Carpathian region of Ukraine.

Depth, km	Velocity of *P* wave, km/s	Velocity of *S* wave, $km\,s^{-1}$	Density, $kg\,m^{-3}$
0	4.70	2.71	2.6
2.5	5.50	3.17	3.18
6.5	6.30	3.64	3.37
8.0	6.10	3.52	3.54
12.0	6.70	3.87	3.76
17.5	6.85	3.95	3.85
21.0	6.40	3.70	4.08
26.5	8.10	4.68	4.37

GID
4, 109–164, 2014

Table 2. Input data for determining the focal mechanism by the traditional graphical method.

Stations	Sign of first arrival	Azimuth,°	Take-off angle,°	lg As/Ap
MEZ	–	265.1	29	0.48
NSLU	+	217.2	29	0.72
RAKU	+	156.4	29	0.33
BRIU	+	250.7	29	1.28
KORU	+	231.6	29	0.53
SHIU	–	335.8	35	0.58
MUKU	–	264.7	35	0.41
BERU	+	249.9	35	0.35
STZU	–	301.7	35	

GID
4, 109–164, 2014

GID
4, 109–164, 2014

Table 3. Parameters of the focal mechanism (Fig. 3) determined by the graphical method.

Plane1			Plane2			*P*		*T*		*N*	
Strike (ϕ_s)	Dip (δ)	Slip (λ)	Strike (ϕ_s)	Dip (δ)	Slip (λ)	Azm	Plunge	Azm	Plunge	Azm	Plunge
243°	72°	69°	114°	27°	138°	349°	24°	125°	58°	250°	20°

Table 4. Spectral parameters for the event near NNP "Synevyr" (6 January 2012) calculated by Eqs. (12)–(19).

M_0, $N \times m$	f_{cp}, Hz	R, m	A, m^2	$\overline{D}$, m	$\Delta\sigma$, MPa	E_s, J	ML
2.1255×10^{12}	7.22	235.1929	1.7378×10^5	5.2204×10^{-4}	0.07147	3.4007×10^7	1.96

GID
4, 109–164, 2014

Table 5. Parameters of the focal mechanism (Fig. 5) determined by the trial and error method.

Plane1			Plane2			P		T		N	
Strike (ϕ_s)	Dip (δ)	Slip (λ)	Strike (ϕ_s)	Dip (δ)	Slip (λ)	Azm	Plunge	Azm	Plunge	Azm	Plunge
251°	80°	82°	112°	13°	130°	169°	35°	331°	54°	253°	9°

GID
4, 109–164, 2014

Table 6. Input data for the determining the focal mechanism by the traditional graphical method.

Stations	Sign of first arrival	Azimuth °	Take-off angle °	lg As/Ap
MEZ	–	263.6	29	0.49
NSLU	+	216.9	29	0.8
BRIU	+	250.2	29	1.32
KORU	+	231.2	29	0.63
SHIU	–	335.6	35	–
MUKU	–	264.2	35	0.5
BERU	+	249.5	35	0.48
STZU	–	301.4	35	0.35

GID
4, 109–164, 2014

Table 7. Parameters of the focal mechanism (Fig. 7) determined by the graphical method.

Plane1			Plane2			P		T		N	
Strike (ϕ_s)	Dip (δ)	Slip (λ)	Strike (ϕ_s)	Dip (δ)	Slip (λ)	Azm	Plunge	Azm	Plunge	Azm	Plunge
104°	27°	129°	241°	69°	72°	345°	22°	125°	62°	248°	17°

GID
4, 109–164, 2014

Table 8. Spectral parameters for the event near NNP "Synevyr" (10 January 2012) calculated by Eqs. (12)–(19).

M_0, $N \times m$	f_{cp}, Hz	R, m	A, m^2	$\overline{D}$, m	$\Delta\sigma$, MPa	E_s, J	ML
6.4227×10^{12}	6.25	271.6949	2.3191×10^5	1.2×10^{-3}	0.1401	1.027×10^8	2.23

GID
4, 109–164, 2014

Table 9. Parameters of the focal mechanism (Fig. 9) determined by the trial and error method.

Plane1			Plane2			*P*		*T*		*N*	
Strike (ϕ_s)	Dip (δ)	Slip (λ)	Strike (ϕ_s)	Dip (δ)	Slip (λ)	Azm	Plunge	Azm	Plunge	Azm	Plunge
255°	80°	82°	116°	13°	130°	173°	35°	331°	54°	257°	8°

GID
4, 109–164, 2014

Determining the focal mechanisms

A. Pavlova et al.

Table 10. Input data for the determining the focal mechanism by the traditional graphical method.

Stations	Sign of first arrival	Azimuth.°	Take-off angle.°	lg As/Ap
NSLU	–	283	−11	0.29
KORU	+	268	29	1.06
MEZ	–	345	29	0.44
RAKU	–	112	29	0.56
BRIU	+	292	29	0.69
TRSU	+	261	29	0.82
BERU	+	276	29	0.75
MUKU	+	294	29	0.72

GID
4, 109–164, 2014

Table 11. Parameters of the focal mechanism (Fig. 11) determined by the graphical method.

Plane1			Plane2			P		T		N	
Strike (ϕ_s)	Dip (δ)	Slip (λ)	Strike (ϕ_s)	Dip (δ)	Slip (λ)	Azm	Plunge	Azm	Plunge	Azm	Plunge
170°	27°	131°	316°	67°	75°	201°	65°	57°	21°	322°	13°

GID
4, 109–164, 2014

Table 12. Spectral parameters for the event near village Ugla (24 October 2012) calculated by Eqs. (12)–(19).

M_0, $N \times m$	f_{cp}, Hz	R, m	A, m^2	$\overline{D}$, m	$\Delta\sigma$, MPa	E_s, J	ML
1.8470×10^{12}	8.25	205.8295	1.3310×10^5	5.9231×10^{-4}	0.009266	2.9552×10^7	1.92

Discussion Paper | Discussion Paper | Discussion Paper | Discussion Paper |
GID
4, 109–164, 2014
Determining the focal mechanisms
A. Pavlova et al.

GID
4, 109–164, 2014

Table 13. Parameters of the focal mechanism (Fig. 13) determined by the trial and error method.

Plane1			Plane2			*P*		*T*		*N*	
Strike (ϕ_s)	Dip (δ)	Slip (λ)	Strike (ϕ_s)	Dip (δ)	Slip (λ)	Azm	Plunge	Azm	Plunge	Azm	Plunge
169°	19°	121°	316°	64°	80°	235°	28°	32°	60°	321°	9°

Table 14. Input data for the determining the focal mechanism by the traditional graphical method.

Stations	Sign of first arrival	Azimuth.°	Take-off angle.°	lg As/Ap
NSLU	+	269	−53	–
KORU	–	260	31	0.43
MEZ	–	6	31	0.084
BRIU	–	295	42	0.65
TRSU	–	253	42	0.57
BERU	e	274	42	2.64
MUKU	–	297	42	0.71
UZH	–	299	45	0.88

GID
4, 109–164, 2014

Table 15. Parameters of the focal mechanism (Fig. 15) determined by the graphical method.

Plane1			Plane2			*P*		*T*		*N*	
Strike (ϕ_s)	Dip (δ)	Slip (λ)	Strike (ϕ_s)	Dip (δ)	Slip (λ)	Azm	Plunge	Azm	Plunge	Azm	Plunge
174°	45°	173°	269°	85°	45°	33°	27°	142°	34°	274°	44°

GID
4, 109–164, 2014

Determining the focal mechanisms

A. Pavlova et al.

Table 16. Spectral parameters for the event 4 April 2013 at 21:15:1436 (ϕ = 48.19774, λ = 23.4663) near the village Nyzhnje Selyshche calculated by Eqs. (12)–(19).

M_0, $N \times m$	f_{cp}, Hz	R, m	A, m^2	$\overline{D}$, m	$\Delta\sigma$, MPa	E_s, J	ML
6.6874×10^{12}	6.81	213.191	1.4271×10^{5}	2.85×10^{-3}	0.302	1.07×10^{8}	2.22

GID
4, 109–164, 2014

Table 17. Parameters of the focal mechanism (Fig. 17) determined by the trial and error method.

Plane1			Plane2			*P*		*T*		*N*	
Strike (ϕ_s)	Dip (δ)	Slip (λ)	Strike (ϕ_s)	Dip (δ)	Slip (λ)	Azm	Plunge	Azm	Plunge	Azm	Plunge
267°	87°	47°	174°	43°	176°	30°	29°	322°	34°	270°	43°

GID
4, 109–164, 2014

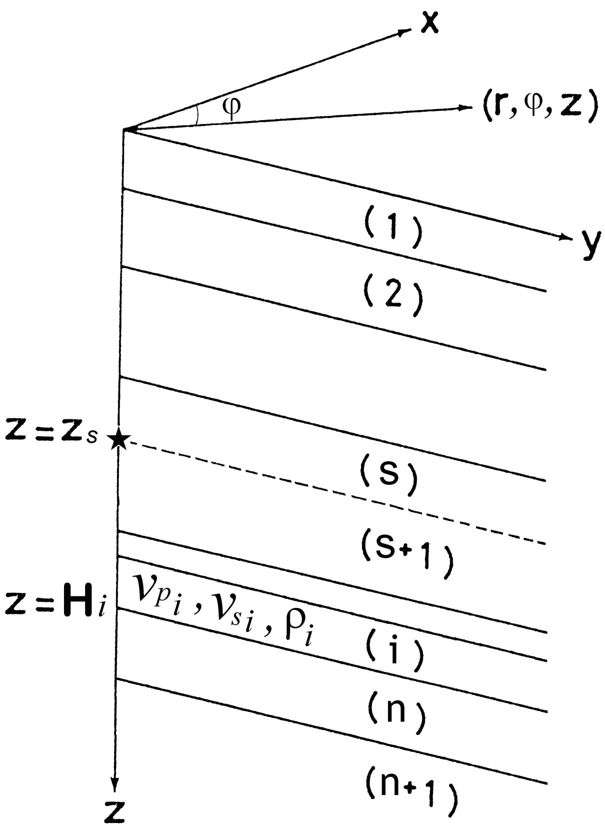

Fig. 1. Model vertically inhomogeneous medium.

GID
4, 109–164, 2014

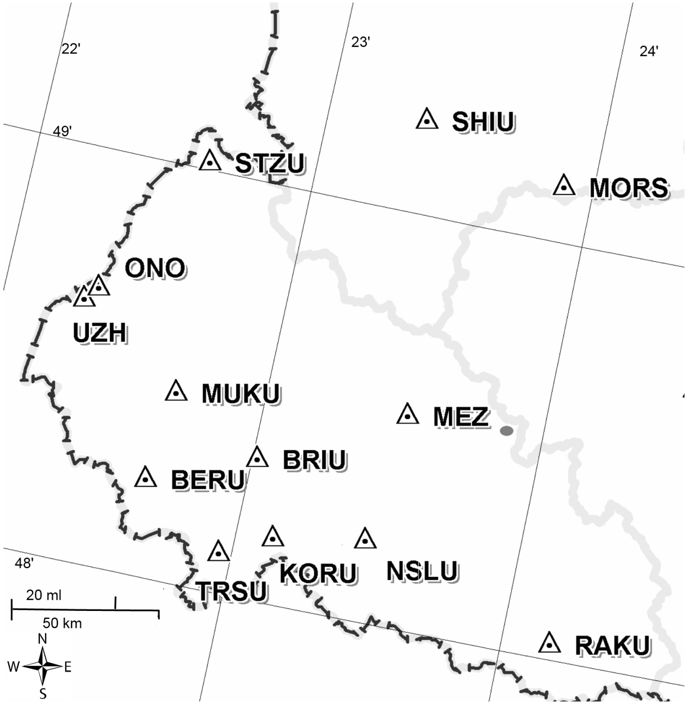

Fig. 2. Location map of the projection of seismic stations in the Carpathian region of Ukraine and specified epicenter of the event near NNP "Synevyr", which took place on 6 January 2012.

GID
4, 109–164, 2014

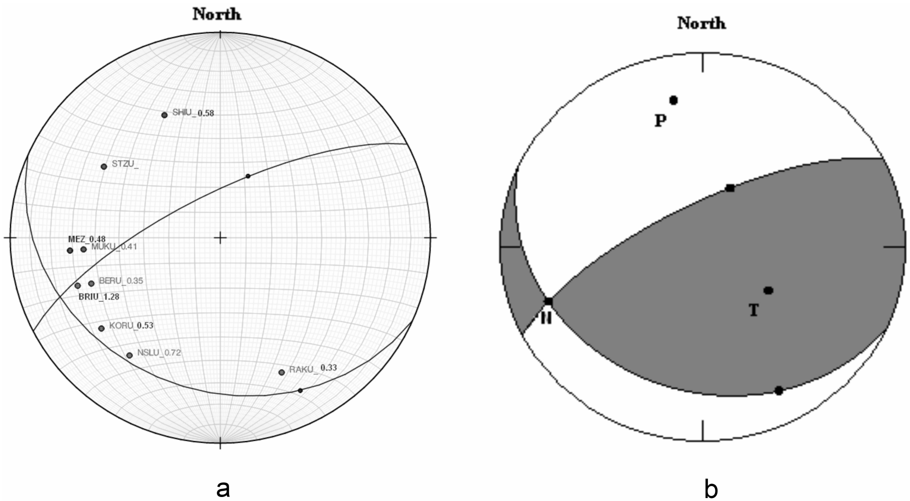

Fig. 3. (a) location of the projection of seismic stations and nodal planes according to the input data (Table 2), **(b)** focal mechanism determined by the graphical method.

GID
4, 109–164, 2014

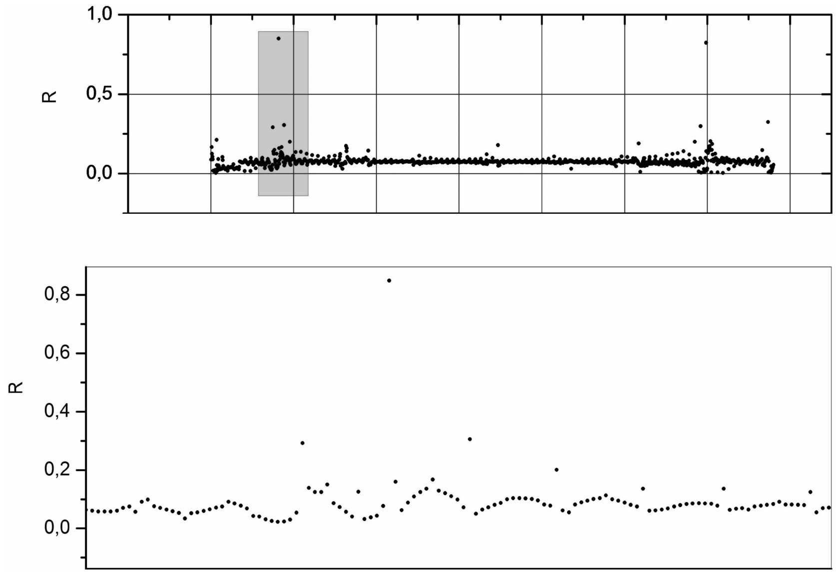

Fig. 4. The correlation coefficients for the event which took place near NNP "Synevyr" on 6 January 2012.

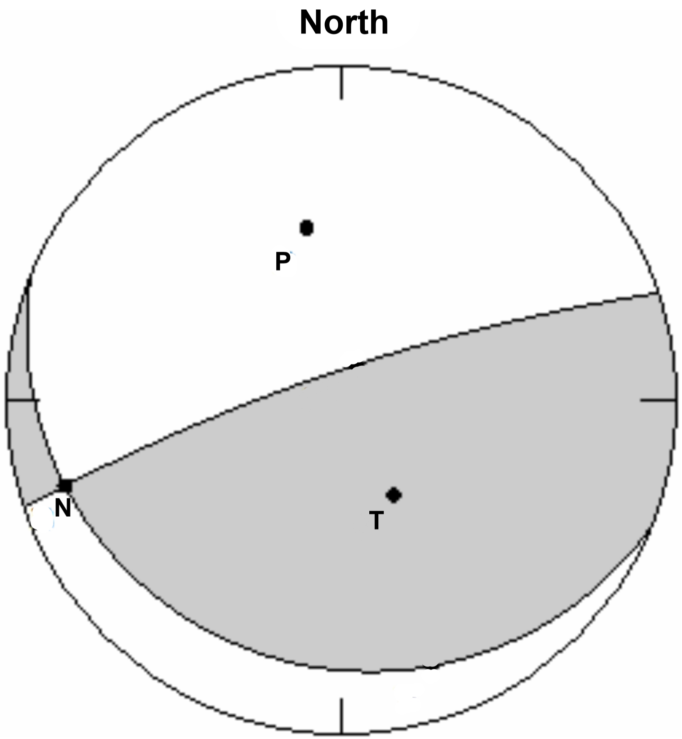

Fig. 5. The focal mechanism determined by the trial and error method.

GID
4, 109–164, 2014

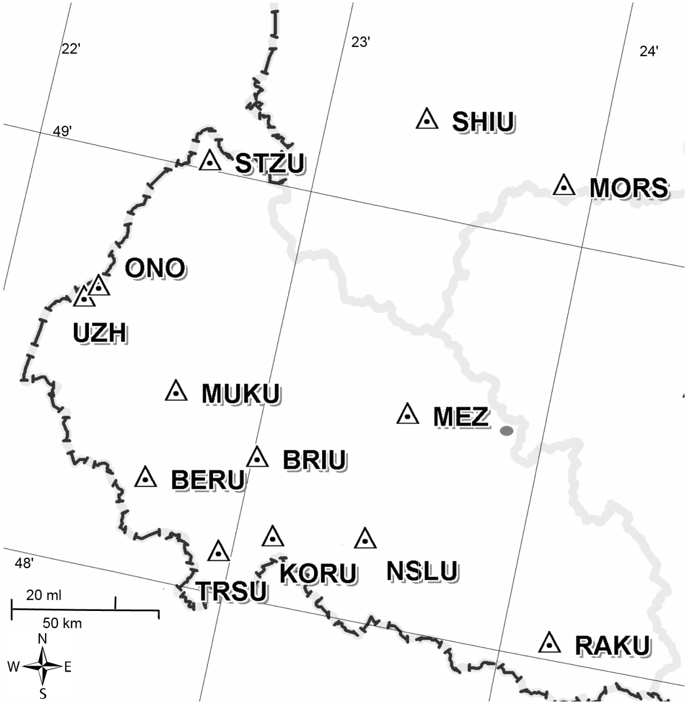

Fig. 6. Location map of the seismic stations in the Carpathian region of Ukraine and specified epicenter of the event near NNP "Synevyr", which took place on 10 January 2012.

GID
4, 109–164, 2014

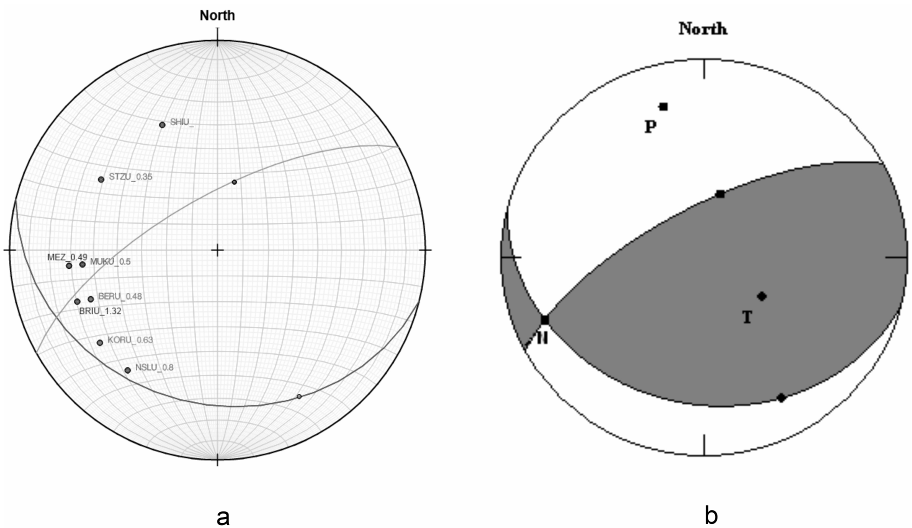

Fig. 7. (a) – location of the projection of seismic stations and nodal planes according to the input data (Table 6), **(b)** – focal mechanism determined by the graphical method.

GID
4, 109–164, 2014

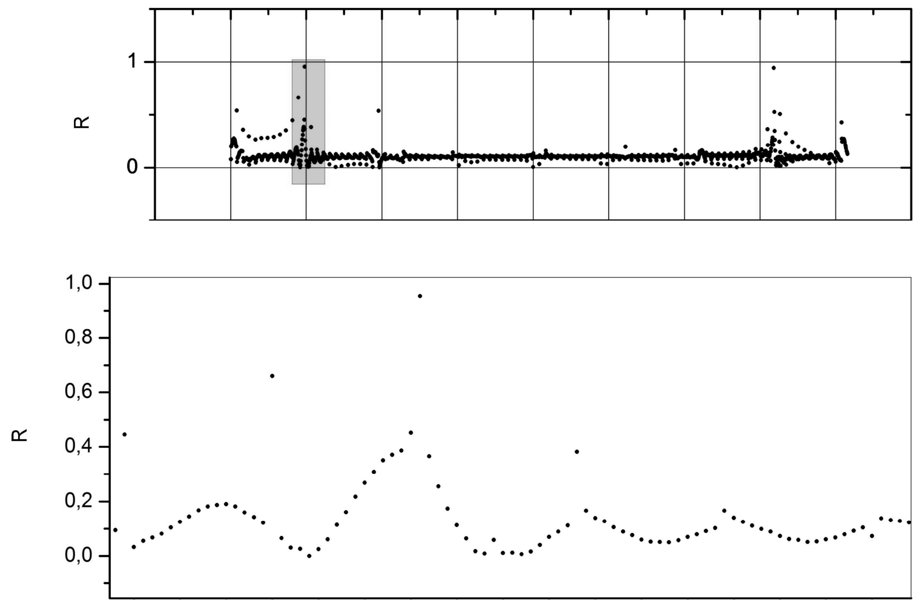

Fig. 8. The correlation coefficients for the event which took place near NNP "Synevyr" on 10 January 2012.

GID
4, 109–164, 2014

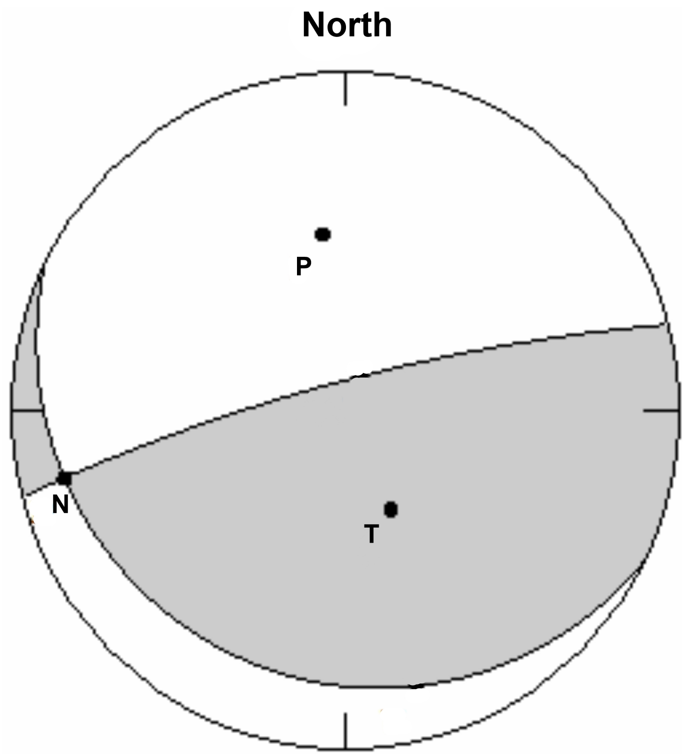

Fig. 9. The focal mechanism determined by the trial and error method for the event near NNP "Synevyr" on 10 January 2012.

GID
4, 109–164, 2014

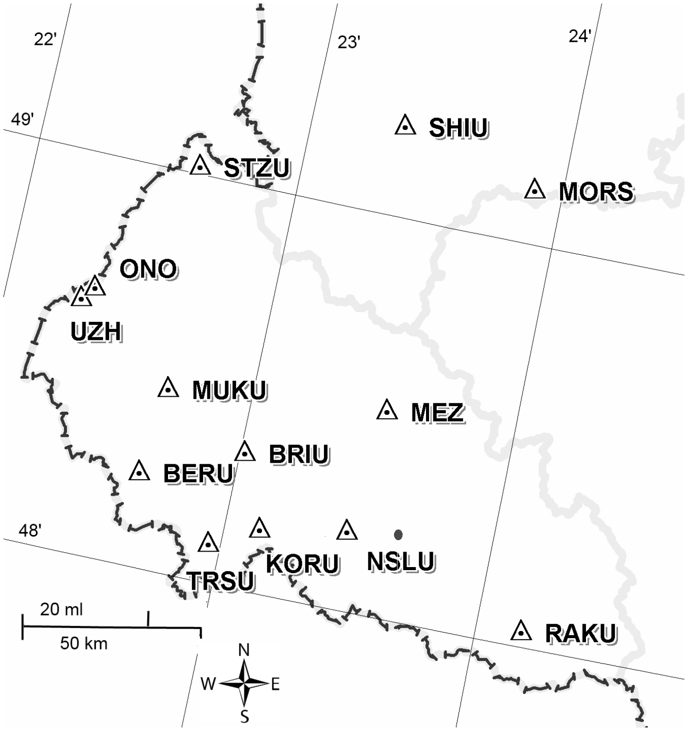

Fig. 10. Location map of the seismic stations in the Carpathian region of Ukraine and specified epicenter of the event near village Ugla, which took place ($\phi = 48.1676°$, $\lambda = 23.6525°$) 24 October 2010 at 03:13:40.501.

GID
4, 109–164, 2014

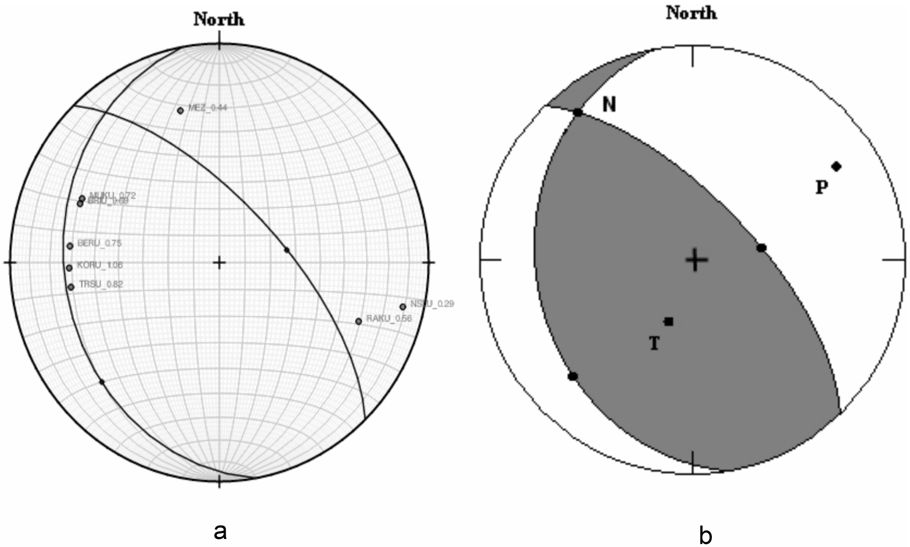

Fig. 11. (a) location of the projection of seismic stations and the nodal planes according to the input data (Table 10), **(b)** focal mechanism determined by the graphical method.

GID
4, 109–164, 2014

Determining the focal mechanisms

A. Pavlova et al.

Title Page
Abstract | Introduction
Conclusions | References
Tables | Figures
◀I | ▶I
◀ | ▶
Back | Close
Full Screen / Esc
Printer-friendly Version
Interactive Discussion

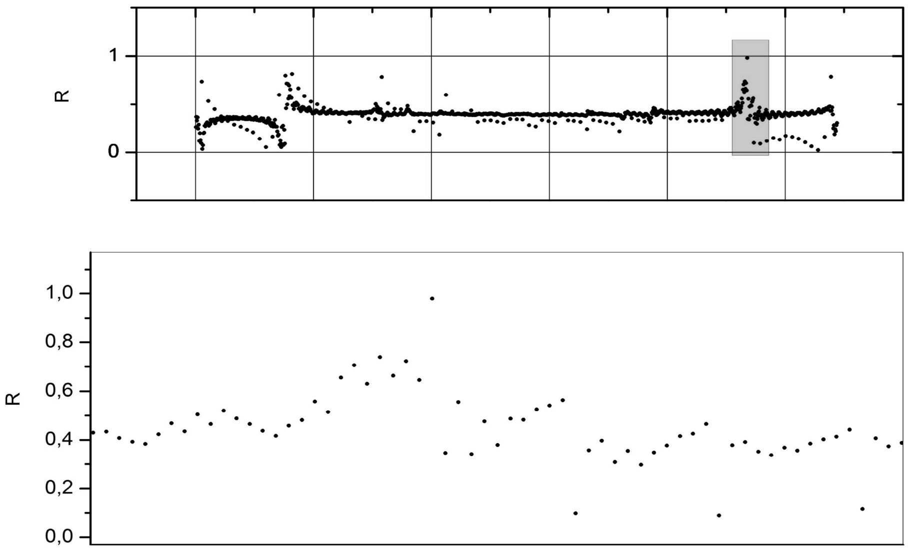

Fig. 12. The correlation coefficients for the event which took place near village Ugla on 24 October 2012.

GID
4, 109–164, 2014

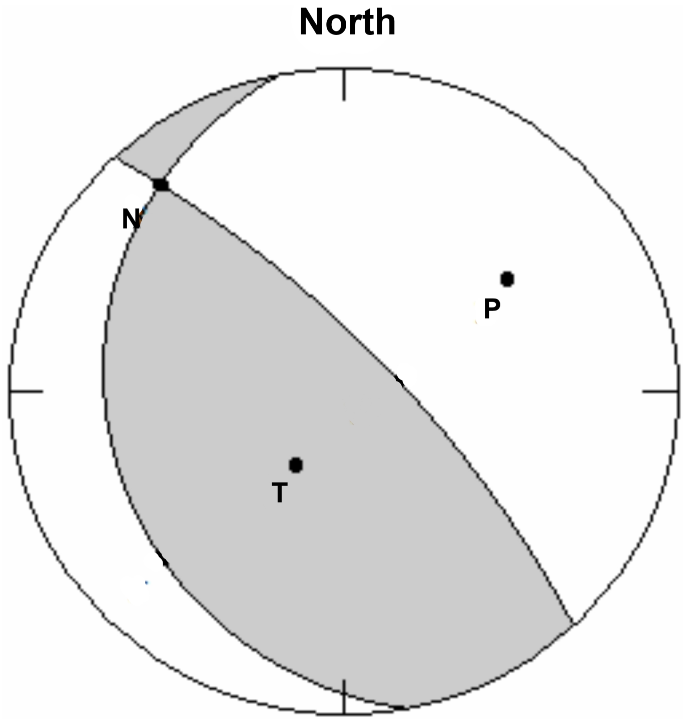

Fig. 13. The focal mechanism determined by the trial and error method.

GID
4, 109–164, 2014

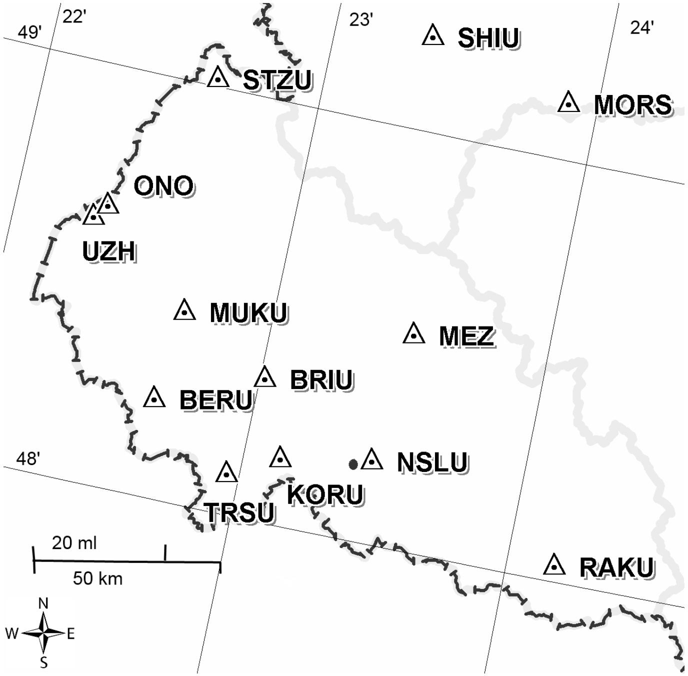

Fig. 14. Location map of the seismic stations in the Carpathian region of Ukraine and specified epicenter of the near village Nyzhnje Selyshche ($\phi = 48.1977°$, $\lambda = 23.4663°$), 4 April 2013 at 21:15:1436.

GID
4, 109–164, 2014

Determining the focal mechanisms

A. Pavlova et al.

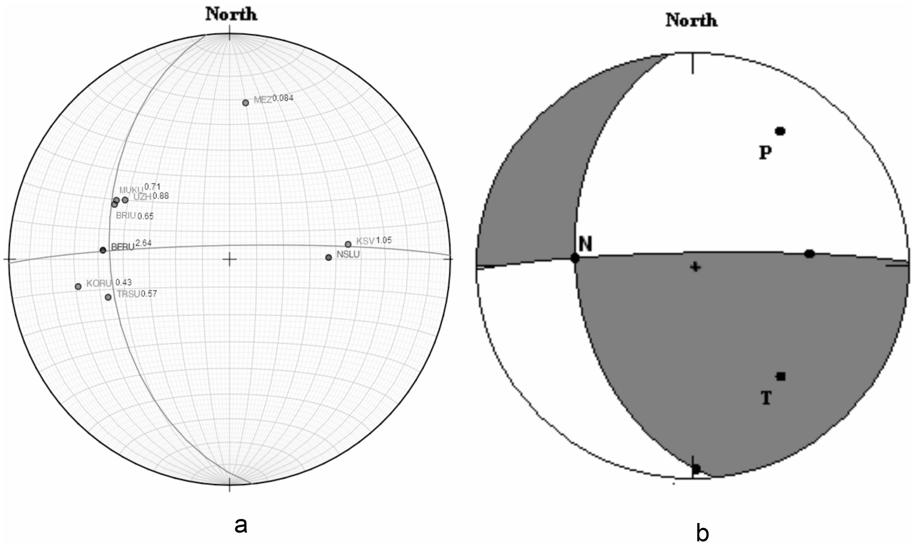

Fig. 15. (a) location of the projection of seismic stations and nodal planes according to the input data (Table 14), **(b)** focal mechanism determined by the graphical method.

GID
4, 109–164, 2014

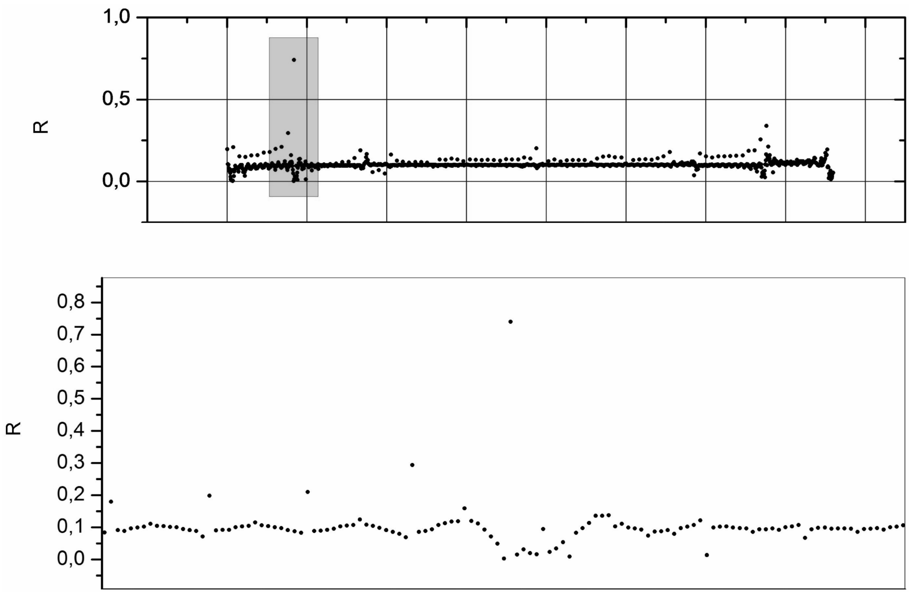

Fig. 16. The correlation coefficients for the event which took place near village Nyzhnje Selyshche on 4 April 2013.

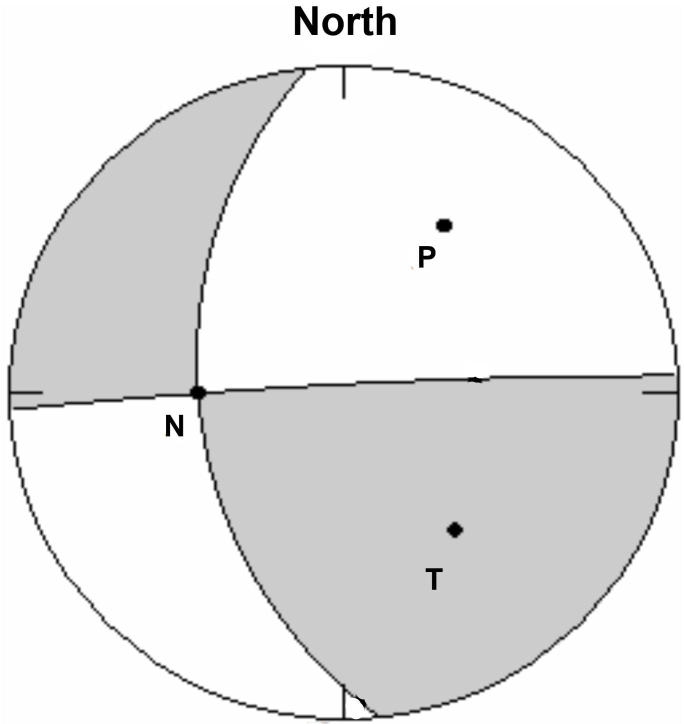

Fig. 17. The focal mechanism determined by the trial and error method.

GID
4, 109–164, 2014

Determining the focal mechanisms

A. Pavlova et al.